Open Access Full Text Article

ORIGINAL RESEARCH

Circular RNA circHUWE1 Is Upregulated and Promotes Cell Proliferation, Migration and Invasion in Colorectal Cancer by Sponging miR-486

Hong-Yu Chen [ID]
Xiang-Nan Li [ID]
Chun-Xiang Ye [ID]
Zhi-Lei Chen [ID]
Zhen-Jun Wang [ID]

Department of General Surgery, Beijing Chao-Yang Hospital, Capital Medical University, Beijing 100020, People's Republic of China

Background: Emerging studies have revealed that circular RNAs (circRNAs) correlate with diverse diseases including cancers. However, little is known about the functions of circRNAs in colorectal cancer (CRC). In our previous research, downregulation of hsa_circ_0140388 (circHUEW1) has been detected in CRC tissues through high-throughput sequencing. However, the underlying mechanism by which circHUWE1 regulates the proliferation and apoptosis in CRC has not been investigated.

Materials and Methods: The levels of circHUWE1 in 58 pairs of CRC tissues and corresponding adjacent healthy tissues were detected by RT-qPCR. In addition, the effects of circHUWE1 on cell proliferation, apoptosis migration and invasion were evaluated by cell proliferation assays, flow cytometry, and transwell assays in HCT116 and SW480 cell lines respectively. Meanwhile, the dual-luciferase reporter system assay was used to explore the interaction between circHUWE1 and miR-486 (hsa-miR-486-5p).

Results: In this study, we demonstrate that the expression of circHUEW1 is upregulated in CRC tissues. High expression of circHUEW1 was significantly associated with lymphovascular invasion ($P =0.036$), lymph node metastasis ($P =0.017$), distant metastasis ($P =0.024$), and TNM stage ($P =0.009$). Moreover, the area under the curve (AUC) of the receiver operating characteristic (ROC) curve was 0.732, which indicated that circHUWE1 could serve as a potential biomarker in the detection of CRC. Silencing circHUWE1 significantly inhibited the proliferation, migration and invasion capacity of CRC cells in vitro. Mechanistically, we demonstrated that circHUWE1 could sponge miR-486 and the downregulation of miR-486 could reverse the cancer suppressive effects caused by silencing circHUWE1.

Conclusion: In this study, our results revealed that circHUWE1 may be a potential therapeutic target and diagnostic biomarker for CRC.

Keywords: circular RNAs, colorectal cancer, hsa_circ_0140388, microRNA sponge, biomarker

Introduction

Colorectal cancer (CRC) mortality was ranked second and CRC incidence was ranked third worldwide among commonly diagnosed cancers according to the latest global cancer statistics in 2018.[1] Although the therapeutic and diagnostic approaches for CRC have improved, the prognosis of patients with CRC remains poor, especially in those with advanced CRC. Thus, it is essential to identify other unclear molecular mechanisms underlying CRC tumorigenesis.

Correspondence: Zhen-Jun Wang
Department of General Surgery, Beijing Chao-Yang Hospital, Capital Medical University, No. 8 Gongtinan Road, Chaoyang District, Beijing 100020, People's Republic of China
Email drzhenjun@163.com

Circular RNAs (circRNAs) are mainly produced from precursor mRNA via back-splicing where an upstream 3′ splice is joined with a downstream 5′ splice.[2,3] Emerging studies have revealed numerous potential functions of circRNAs including acting as microRNA (miRNA) sponges, regulating transcription and splicing, sequestrating RNA binding proteins, and protein-coding capacity.[4–7] Based on the above functions of circRNAs above, a number of studies have revealed that circRNAs correlate with diverse diseases,[8–11] including cancers.[12–15] Thus, circRNAs hold the potential to function as therapeutic targets and diagnostic biomarkers of cancers. However, little is known regarding to the functions of circRNAs in CRC.

In our previous study, we used high-throughput sequencing to identify differently expressed circRNAs between 4 matched CRC tissues and their adjacent tissues.[16] The expression level of circHUWE1 (hsa_circ_0140388) was higher in CRC tissues. The circHUWE1 is derived from HUWE1 (HECT, UBA and WWE domain containing E3 ubiquitin protein ligase 1; hsa_circ_0140388; Figure 1) and is located on chromosome X (53641494-53644407). The spliced length of circ_0140388 is 589 base pairs. In this study, we determined the expression level of circHUWE1 in CRC tissues using quantitative real-time polymerase chain reaction (qRT-PCR), and analyzed the correlation between circHUWE1 level and the clinicopathologic features of CRC patients. The results of qRT-PCR showed that circHUWE1 was up-regulated in CRC tissues and the

circHUWE1 level was correlated with unfavorable clinicopathologic features. The area under the curve (AUC) of the receiver operating characteristic (ROC) was 0.732, which indicated that circHUWE1 could serve as a potential biomarker in the detection of CRC.

To further explored the biological function of circHUWE1 in CRC progression, in vitro assays were performed. The loss-of-function assays performed in HCT116 and SW480 cell lines revealed that silencing circHUWE1 significantly inhibited the capacity of proliferation, colony forming, migration and invasion and promoted apoptosis of CRC cells.

To explore the possible mechanism underlying the cancer promoting properties of circHUWE1 in CRC, bioinformatics analyses were performed. The results analyzed using miRanda software suggested that circHUWE1 could potentially bind to hsa-miR-486-5p (miR-486) which was down-regulated in CRC tissues and was associated with an unfavorable overall survival according to The Cancer Genome Atlas (TCGA) database.

Furthermore luciferase reporter assay verified the interaction between circHUWE1 and miR-486. The tumor-inhibiting effect of silencing circHUWE1 was reversed by the down-regulation of miR-486. Taken together, the above results demonstrate that circHUWE1 exerts cancer promoting effects in CRC by sponging miR-486. In conclusion, our study showed that circHUWE1 was significantly up-regulated CRC tissues and the expression level
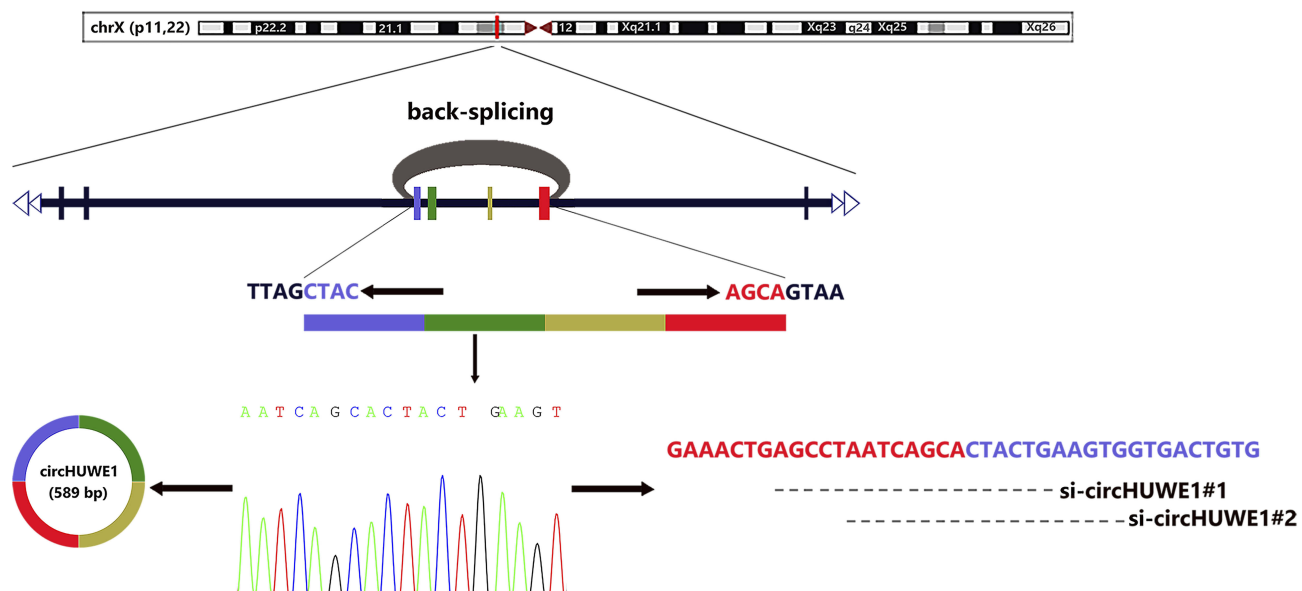

Figure 1 Biogenesis, Sanger sequencing result and designed siRNAs of circHUWE1. Schematic diagram shows that circHUWE1 is derived from exon 20–23 of HUWE1 gene via back-splicing. The back-splice junction sequences of circHUWE1 was verified by Sanger sequencing. Two siRNAs targeting the back-splice junction site of circHUWE1 were designed.

of circHUWE1 was associated with unfavorable clinico-pathologic features. As circHUWE1 exerts cancer promoting effects in CRC by sponging miR-486, circHUWE1 may serve as a potential diagnostic biomarker and therapeutic target for CRC.

Materials and Methods
Patients and Specimens

A total of 58 CRC tissues and corresponding adjacent healthy tissues were obtained from patients in Beijing Chao-Yang Hospital, Capital Medical University between 2017 and 2019. All surgical tissue specimens were immediately frozen in liquid nitrogen and stored at −80°C for further use. All CRC specimens were confirmed pathologically, and none of the patients had received preoperative chemotherapy, radiotherapy or targeted therapy. Written informed consents were obtained from all patients. The present study was approved by the Ethics Committee of the Beijing Chao-Yang Hospital, Capital Medical University and was carried out in accordance with the ethical standards formulated in the Helsinki Declaration.

Cell Culture

All cell lines including HCT116, SW480 and HEK-293T were obtained from the American Type Culture Collection (Manassas, VA, USA). HCT116 cells were cultured in McCoy's 5A Modified Medium (Biological Industries, Israel). The other cells were cultured in Dulbecco's Modified Essential Medium (Biological Industries, Israel). The media were supplemented with 100 U/mL penicillin, 100 μg/mL streptomycin and 10% fetal bovine serum. All cells were grown in a humidified atmosphere with 5% CO_2 at 37°C.

RNA Extraction and Quantitative Real-Time PCR

Total RNA was isolated from the cells and tissues using TRIzol (Invitrogen, Carlsbad, CA, USA) according to the manufacturer's protocol and then stored at −80°C. For circRNA, total RNA was reverse transcribed into cDNA using the PrimeScript™ RT reagent Kit (TaKaRa, Dalian, China). Real-time PCR was then conducted using TB Green™Premix Ex Taq™ II (TaKaRa, Dalian, China). 18S rRNA was selected as an internal control. Real-time PCR was conducted using the ABI 7500 real-time PCR system (Applied Biosystems, Foster City, CA, USA). We designed specific divergent primer to span the backsplice

junction site of circHUWE1. Primer sequences were synthesized as follows: circHUWE1 forward: 5′-CCCCCA AGGTCTAATCATGCC-3′, reverse: 5′- ACATTTGGGAG GGAGCCAAG-3′. 18S rRNA forward primer: 5′-AAACG GCTACCACATCCA-3′, reverse primer: 5′-CACCAGAC TTGCCCCTCCA-3′. All the primers were synthesized by Sangon Biotech (Shanghai, China). The relative expression of the RNAs was calculated by the $2^{-\Delta\Delta Ct}$ method.

TCGA Database Analysis

The miRNA expression information and related clinical information of colorectal cancer samples were downloaded from the GDC data portal (https://portal.gdc.cancer.gov/) and analyzed by R Studio. The data contained 531 tumor samples and 11 normal samples. The edgeR package (http://bioconductor.org/packages/release/bioc/html/edgeR.html) was used to screen differentially expressed miRNAs between CRC and normal tissues. A |logFC|>5 and adjusted P-value <0.05 were set as the cut-off criteria. Then Kaplan–Meier survival analysis was performed to determine whether the expression levels of the differentially expressed miRNAs correlated with the prognosis of CRC.

Analyses of circHUWE1-miRNA Interaction in CRC

We used miRanda software (v3.3a) to predict target miRNAs of circHUWE1 under the setting parameters described previously(Gap Open Penalty: −9; Gap Extend Penalty: −4; Score Threshold: 140; Energy Threshold: −20 kcal/mol; Scaling Parameter: 4).[17] The results of the TCGA analysis were used to further screen the target miRNAs.

Transfection

Small interfering RNA (siRNA), miR-486 mimics, and miR-486 inhibitors, as well as their respective negative control oligonucleotides were purchased from GenePharma (Shanghai, China). HCT116 and SW480 cells were transfected with the oligonucleotides at a final concentration of 50 nM using the Lipofectamine 3000 (Invitrogen, Carlsbad, CA, USA) according to the instructions provided by the manufacturer. The sequences were as follows: si-circHUWE1#1: 5′-CAGUAGUGCUGAUUAG GCUTT-3′; circHUWE1#2: 5′- CACUUCAGUAGUGCU GAUUTT-3′; negative control: 5′-TTCTCCGAACGTGT CACGT-3′.

Dual Luciferase Reporter Assay

For circHUWE1 and miR-486, circHUWE1 sequence containing wild-type or mutant miR-486 binding sites were synthesized and inserted into the psiCheck2 luciferase vector (Promega, Madison, WI, USA). Subsequently, the wild or mutant vector was respectively co-transfected with miR-486 mimics or the negative control into HEK-293T cells using the Lipofectamine 3000 (Invitrogen, Carlsbad, CA, USA). The luciferase activity was tested 48 h later using the Dual-Luciferase Reporter Assay System (Promega, Madison, WI, USA).

Colony Formation Assay

SW480 or HCT116 cells were seeded into 6-well plates 24 h after transfection. Approximately two weeks post-seeding, the colonies were fixed using 4% paraformaldehyde for 20 min, and then stained using 0.1% Crystal Violet for 20 min. The colonies were photographed and analyzed.

Cell Proliferation Analysis

Cell viability was determined using CCK-8 (Cell Counting Kit-8) according to the manufacturer's instructions. Approximately 1×10^3 cells in logarithmic growth phase were collected and then seeded into 96-well plates. Ten μL CCK-8 reagent (Dojindo Laboratories, Kumamoto, Japan) was added to each well at 0, 24, 48, 72 and 96 h after the cells were seeded. The cells were incubated for 2 h, and a Varioskan Flash Spectral Scanning Multimode Reader (Thermo Fisher Scientific, Waltham, MA, USA) was then used to measure the optical density at a wavelength of 450 nm. The data of the OD450 value were used to reflect cell proliferation rates.

Cell Apoptosis Analysis

Following 24 h of transfection, the cells were collected and then re-suspended in binding buffer. Annexin V-FITC and propidium iodide (KeyGen Biotech, Nanjing, China) were added to stain the cells. Flow cytometry was conducted using a FACS Canto II (BD Biosciences, Heidelberg, Germany). The data were collected and analyzed by FCS Express 5 software (DeNovo Software, Los Angeles, CA, USA).

Transwell Assay

To evaluate the properties of migration and invasion, the transwell assay was conducted using the Transwell system (Corning, NY, USA). Following transfection for 24 h, the cells supplemented with serum-free medium were respectively seeded into the upper chambers coated with (for invasion) or without (for migration) Matrigel. The lower chambers contained 500 μL culture medium plus 20% fetal bovine serum. After incubation at 37°C with 5% CO2 for 48 h, the non-migrated or uninvaded cells on the upper chambers were wiped with cotton swabs and the migrated or invaded cells were fixed with 4% paraformaldehyde for 20 min and then stained with 0.1% crystal violet for 20 min. The cells on the lower side of the membrane were observed under a Leica DM4000B microscope (Leica, Wetzlar, Germany). The cell quantification was performed with open-source software (ImageJ; https://imagej.nih.gov/ij/).

RNA Fluorescence in situ Hybridization (FISH)

The FAM-labeled circHUWE1 probe was customized by GenePharma (Shanghai, China). Hybridization was performed overnight using the FISH Kit (GenePharma, Shanghai, China). Images were obtained by Leica Microsystems (Inverted Microscope Solution DMi8 S Platform).

Statistical Analysis

All statistical analyses were performed using SPSS 23.0 (IBM, SPSS, Chicago, IL, USA). Figures were produced using GraphPad Prism 7.0 for Windows (GraphPad Software, Inc. La Jolla, CA, USA) and R studio. The paired *t*-test was used to analyze differences in the levels of hsa_circ_0140388 between CRC tissues and paired adjacent healthy mucosal tissues. The Chi-square test was used to examine the correlation between the clinicopathologic features and the level of circHUWE1 expression. The paired *t*-test was used to analyze the data of in vitro assays. A P value <0.05 was considered statistically significant.

Results
CircHUWE1 Was Up-Regulated and Could Be Served as a Diagnostic Biomarker in CRC

CircHUWE1 is derived from exon 20–23 of the HUWE1 gene, with a spliced sequence length of 589 base pairs (Figure 1). The expression of circHUWE1 was analyzed by qRT-PCR in 58 pairs of CRC and healthy mucosal tissues to determine whether circHUWE1 was differentially expressed. The expression of circHUWE1 was significantly higher in CRC tissues (Figure 2A). Of the 58 CRC tissues, 77.59% (45/58) showed increased expression of circHUWE1
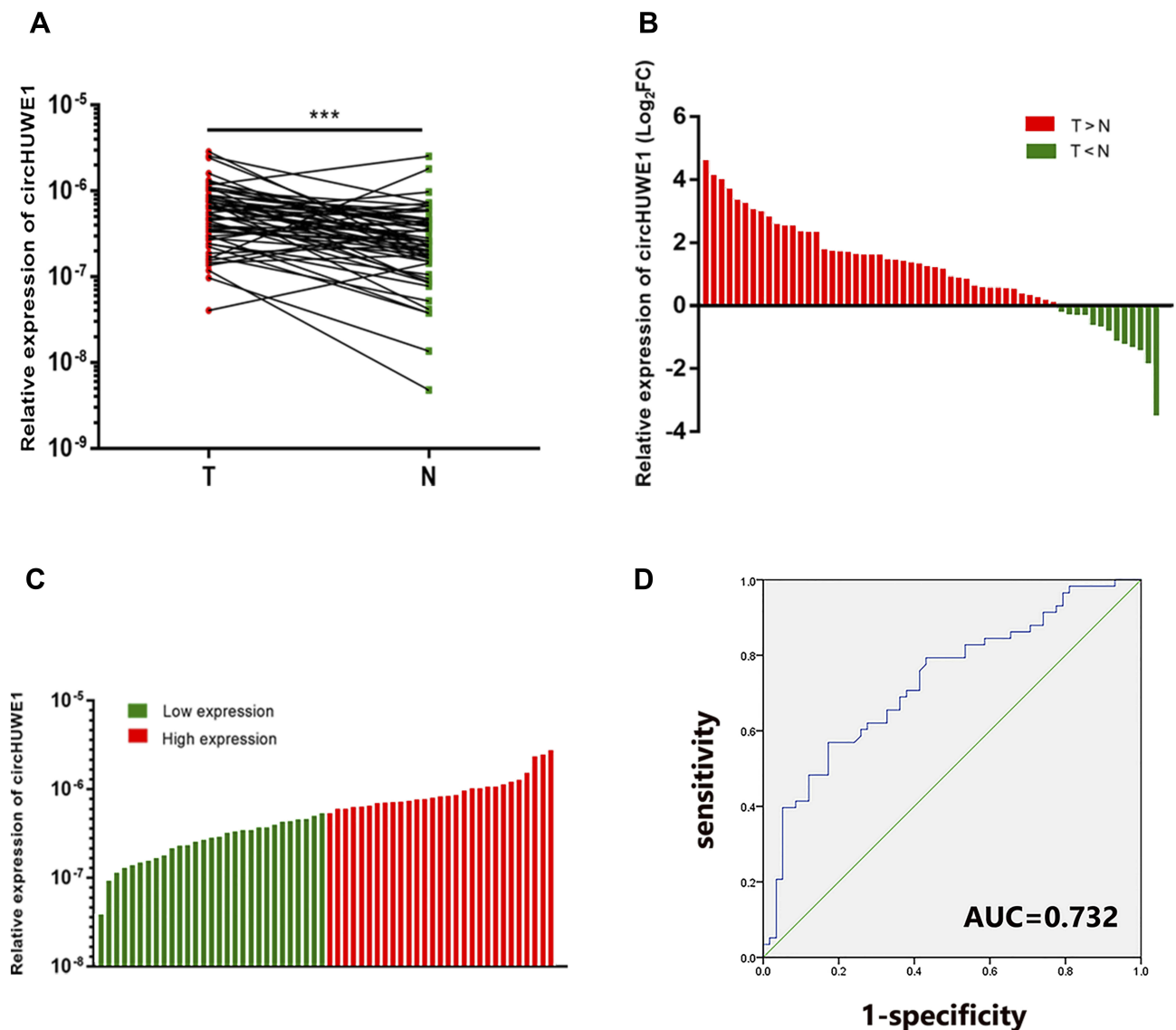
Figure 2 Expression levels of circHUWE1 in CRC tissues. (**A**) The results of qRT-PCR for circHUWE1 in 58 matched pairs of CRC and corresponding adjacent normal tissues showed that circHUWE1 was significantly higher in CRC tissues compared with corresponding adjacent normal tissues. (**B**) 77.59% (45/58) of the 58 CRC tissues showed increased expression (log2FC) of circHUWE1. (**C**) The 58 CRC patients were categorized into low or high expression groups based on the median expression level of circHUWE1. (**D**) ROC curve of circHUWE1 to distinguish CRC from controls. ***p < 0.001.

(Figure 2B). We categorized the level of circHUWE1 in 58 CRC tissues as low or high expression based on the median expression level of circHUWE1 (Figure 2C). The results showed that the level of circHUEW1 was significantly associated with lymphovascular invasion ($P =0.036$), lymph node metastasis ($P =0.017$), distant metastasis ($P =0.024$), and TNM stage ($P =0.009$) (Table 1). Increasing studies have reported that circRNAs have the potential to serve as biomarkers to detect cancer.[18–20] We used the ROC curve to assess the diagnostic value of circHUWE1 for CRC. The AUC was 0.732 (Figure 2D), which showed that circHUWE1 may serve as a potential diagnostic biomarker

for CRC. Taken together, our results suggested that circHUWE1 was highly expressed in CRC and may play a potential functional role in CRC progression.

Confirmation of the Circular Structure and Subcellular Localization of circHUWE1

To confirm the back-splice junction sequences, the qRT-PCR products of circHUWE1 were analyzed by Sanger sequencing, and the results verified the back-splice junction sequences (Figure 1). The RNA FISH analysis indicated that circHUWE1 was predominantly located in the cytoplasm (Figure 3A).

Table 1 Association of circHUWE1 Level with Clinicopathologic Features in CRC Patients

Clinicopathologic Features	Total (n =58)	circHUWE1 Expression[a]				p value
		Low (%)		High (%)		
Gender						
Male	31	15	(48.4%)	16	(51.6%)	0.792
Female	27	14	(51.9%)	13	(48.1%)	
Age (years)						
≤65	32	19	(59.4%)	13	(40.6%)	0.113
> 65	26	10	(38.5%)	16	(61.5%)	
Tumor site						
Colon	37	18	(48.6%)	19	(51.4%)	0.785
Rectum	21	11	(52.4%)	10	(47.6%)	
Tumor size (cm)						
≤5	35	20	(57.1%)	15	(42.9%)	0.18
> 5	23	9	(39.1%)	14	(60.9%)	
Lymphovascular invasion						
Absent	30	19	(63.3%)	11	(36.7%)	0.036*
Present	28	10	(35.7%)	18	(64.3%)	
Differentiation						
Well-moderate	41	22	(53.7%)	19	(46.3%)	0.387
Poor	17	7	(41.2%)	10	(58.8%)	
Depth of invasion						
T1-T2	16	11	(68.8%)	5	(31.3%)	0.078
T3-T4	42	18	(42.9%)	24	(57.1%)	
Lymph node metastasis						
N0	33	21	(63.6%)	12	(36.4%)	0.017*
N1-N2	25	8	(32.0%)	17	(68.0%)	
Distant metastasis						
M0	47	27	(57.4%)	20	(42.6%)	0.019*
M1	11	2	(18.2%)	9	(81.8%)	
TNM stage						
I–II	30	20	(66.7%)	10	(33.3%)	0.009**
III-IV	28	9	(32.1%)	19	(67.9%)	

Notes: *p < 0.05. **p < 0.01. [a]Using median expression level of circHUWE1 as cutoff value.

CircHUWE1 Exerted Oncogenic Properties in CRC Cells

To detect the biological functions of circHUWE1 in the progression of CRC, we performed loss-of-function assays in CRC cell lines. We silenced circHUWE1 expression in the HCT116 and SW480 cell lines. Two siRNAs targeting circHUWE1 were synthesized (Figure 1). qRT-PCR was performed and the results showed that si-circHUWE1#1 had a significant knockdown effect on circHUWE1, but had no effect on HUWE1 mRNA (Figure 4A). Therefore, si-circHUWE1#1 was used in subsequent experiments.

Silencing circHUWE1 significantly inhibited proliferation (Figure 4B), colony formation (Figure 4C), migration and invasion (Figure 4E and F) in these cells. In addition, the apoptotic rate of CRC cells was increased (Figure 4D). The above results revealed that circHUWE1 exerted oncogenic properties in CRC cells, which were consistent with the clinical findings.

CircHUWE1 Promoted CRC Progression by Sponging miR-486

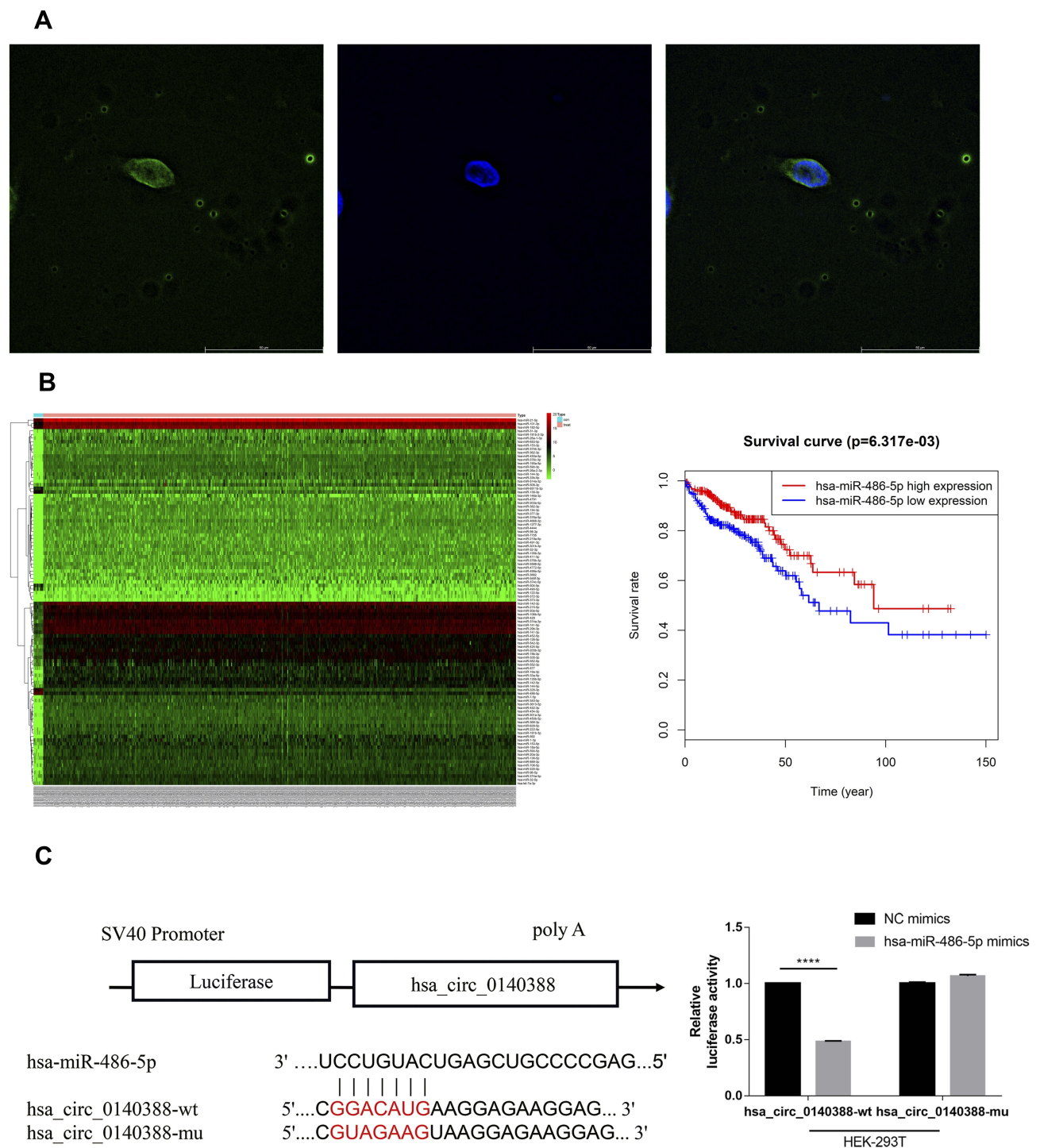Numerous studies have verified that circRNAs are able to function by sponging miRNAs.[13,18,21] Thus, in order to

A

B

Survival curve (p=6.317e-03)

C

SV40 Promoter		poly A
Luciferase	hsa_circ_0140388	

hsa-miR-486-5p   3' ….UCCUGUACUGAGCUGCCCCGAG...5'

hsa_circ_0140388-wt   5'....CGGACAUGAAGGAGAAGGAG... 3'
hsa_circ_0140388-mu   5'....CGUAGAAGUAAGGAGAAGGAG... 3'

Figure 3 The interaction between circHUWE1 and miR-486. (**A**) RNA FISH images showed the distribution of circHUWE1 is dominantly in cytoplasm. (**B**) The heatmap shows the analysis result of differentially expressed miRNAs of the TCGA data (logFC>5), and miR-486 is significantly down-regulated(left). And the Kaplan–Meier survival analysis shows low miR-486 expression level was associated with unfavorable overall survival (P =0.013). (**C**) Schematic diagram of the predicted miR-486 binding site in circHUWE1 and mutant binding site (left). Dual luciferase reporter assay in 293T cells showed miR-486 mimics could significantly inhibit the luciferase activity of the wild-type circHUWE1 luciferase vector, while the luciferase activity of the mutant-type vector did not change. The relative luciferase activities were normalized with Renilla luciferase activity. ****p < 0.0001.

investigate the possible mechanism underlying the cancer promoting properties of circHUWE1 in CRC, we predicted the binding miRNAs of circHUWE1 using miRanda software (v3.3a) (Supplementary data: Data 1). In addition, we used the R program to analyze the miRNA expression data in CRC tissues from the TCGA
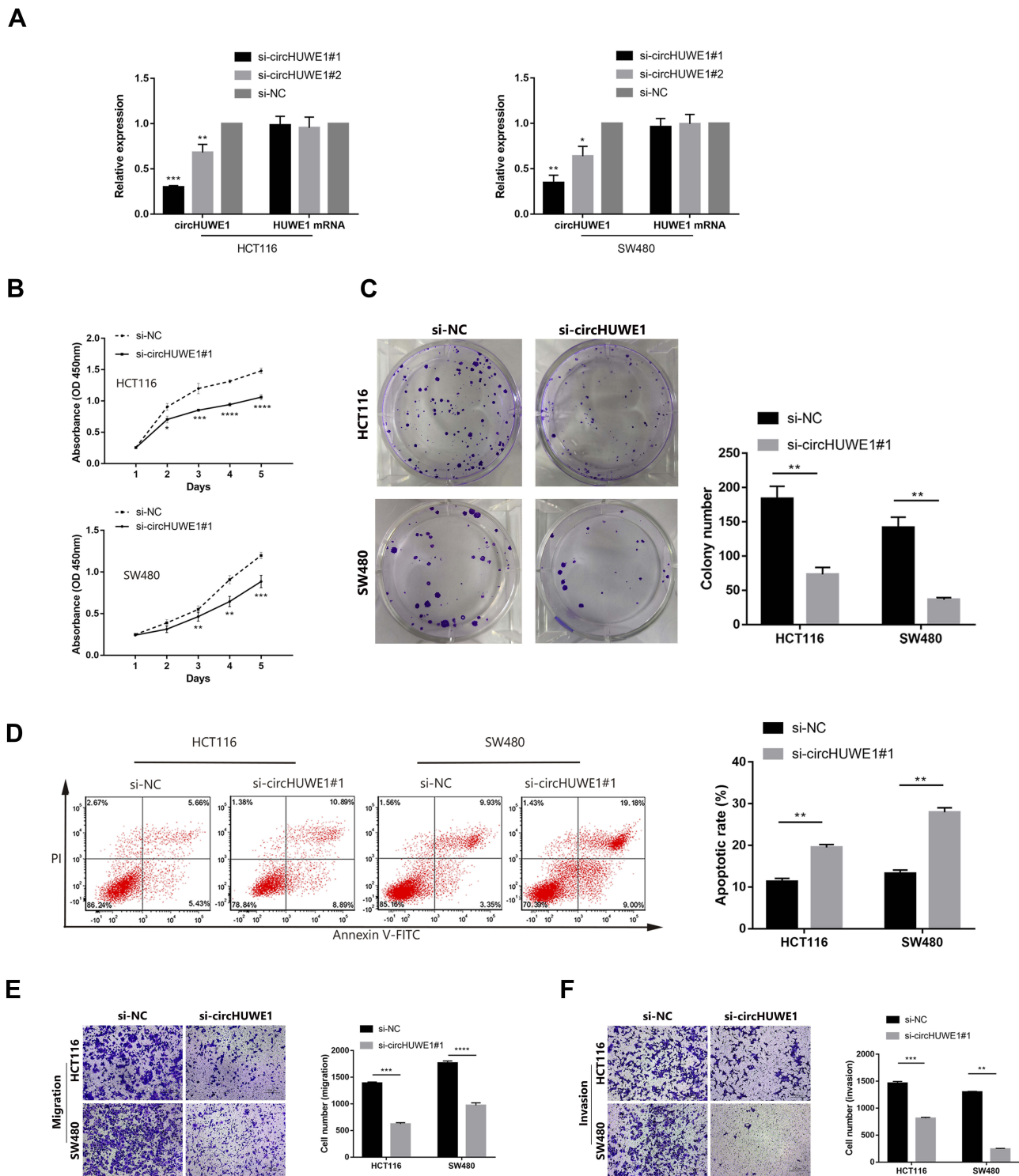
Figure 4 Silencing circHUWE1 inhibited the proliferation, migration and invasion capacity of CRC cells in vitro. (**A**) The expression of circHUWE1 and HUWE1 mRNA in HCT116 and SW480 cells were measured by qRT-PCR after transfected with different siRNAs targeting the back-splice junction site of circHUWE1 or negative control (si-NC). (**B**) CCK-8 assays showed that silencing circHUWE1 inhibited the proliferative ability of HCT116 and SW480 cells. (**C**) Colony formation assays indicated that the colony-forming capacity of HCT116 and SW480 cells was attenuated with silencing circHUWE1. (**D**) Flow cytometry to detect cell apoptosis suggested that HCT116 and SW480 cells with circHUWE1 silencing presented significantly higher apoptotic rate. (**E** and **F**) Transwell assays showed that silencing circHUWE1 significantly inhibited the migration and invasion capacity of HCT116 and SW480 cells. Data are showed as means ± s.d. of at least three independent experiments. *p < 0.05, **p < 0.01, ***p < 0.001, ****p < 0.0001.

430

OncoTargets and Therapy 2020:13

database. The results suggested that among the target miRNAs of circHUWE1, miR-486 was down-regulated in CRC tissues according to the TCGA database (Figure 3B). Furthermore, the results of Kaplan–Meier survival analysis suggested that low expression level of miR-486 was associated with unfavorable overall survival (P =0.013). Moreover, miR-486 has been reported to function as a tumor suppressor in CRC.[22,23]

To further verify the predicted interaction between circHUWE1 and miR-486, we performed a luciferase reporter assay. As shown in Figure 3C, miR-486 mimics significantly inhibited the luciferase activity of the wild-type circHUWE1 luciferase vector, while the luciferase activity of the mutant-type vector did not change.

Based on the results of bioinformatics analyses and luciferase reporter assay, we conducted functional experiments to explore whether miR-486 mediated the role of circHUWE1 in CRC progression. MiR-486 mimics had similar tumor-inhibiting effects to si-circHUWE1#1 (Figure 5A–D). These data suggested that circHUWE1 may exert its tumor-promoting functions by sponging miR-486 in CRC. Reverse experiments were conducted to examine whether miR-486 downregulation could offset the tumor-inhibiting effect of si-circHUWE1#1. The results showed that miR-486 downregulation significantly offset the circHUWE1 down-regulated-mediated inhibition of the proliferation (Figure 6A), migration (Figure 6B) and invasion (Figure 6C) of HCT116 and SW480 cells. Taken together, the above results demonstrated that circHUWE1 exerted cancer promoting effects in CRC by sponging miR-486.

Discussion

CircRNAs were once considered aberrant byproducts of splicing[24] and did not attract much attention. However, due to the advances in biological technology, especially high-throughput sequencing technology and bioinformatics, their abundance in diverse cells has recently been discovered.[25–28] A number of studies have reported that circRNAs play a critical role in many diseases,[8–11] including cancers.[12–15] However, the functions of circRNAs in CRC are unclear. In the present study, we found that circHUWE1 was upregulated in CRC tissues and this was consistent with our previous research on high-throughput sequencing and bioinformatics analyses. Moreover, the expression of circHUEW1 was significantly associated with lymphovascular invasion, lymph

node metastasis, distant metastasis, and TNM stage. The relationship between high expression of circHUWE1 and unfavorable clinical pathological characteristics suggested that circHUWE1 may contribute to the progression of CRC.

Recently, an increasing number of studies have revealed that circRNAs may serve as potential therapeutic targets and diagnostic biomarkers for cancer. In our research, the loss-of-function studies indicated that silencing circHUWE1 significantly inhibited the capacity of proliferation, colony formation, migration and invasion and promoted apoptosis of CRC cells. To further investigate the potential mechanism underlying the cancer promoting effects of circHUWE1 in CRC, a luciferase reporter assay was performed to verify the predicted direct interaction between circHUWE1 and miR-486, and the results confirmed the prediction of miRanda software. Further experiments showed that miR-486 downregulation significantly offset the circHUWE1 down-regulated-mediated inhibition of proliferation, migration and invasion of CRC cells. Thus, our research demonstrated that circHUWE1 exerts cancer promoting effects in CRC by sponging miR-486.

Although we identified that circHUWE1 is a new functional circRNA in CRC progression and exerts its cancer promoting properties by sponging miR-486, some limitations should be noted. Firstly, further investigations into the relationship between miR-486 and its target mRNAs were not performed. It was reported that miR-486 affected CRC progression by targeting PLAGL2 and subsequently inhibiting the PLAGL2/ IGF2/β-catenin signal pathways.[22] Hence, further research is required to assess whether there is a correlation between circHUWE1 and the target mRNA of miR-486. Secondly, although our research showed that circHUWE1 played a role in the progression of CRC by sponging miR-486, it is unclear whether circHUWE1 may function through other pathways, such as regulating transcription or sequestrating RNA binding proteins.

Conclusion

Our study showed that circHUWE1 was significantly up-regulated in CRC tissues and the expression level of circHUWE1 was associated with unfavorable clinico-pathologic features. CircHUWE1 has the capability to serve as a potential diagnostic biomarker for CRC. CircHUWE1 exerted cancer promoting effects in CRC
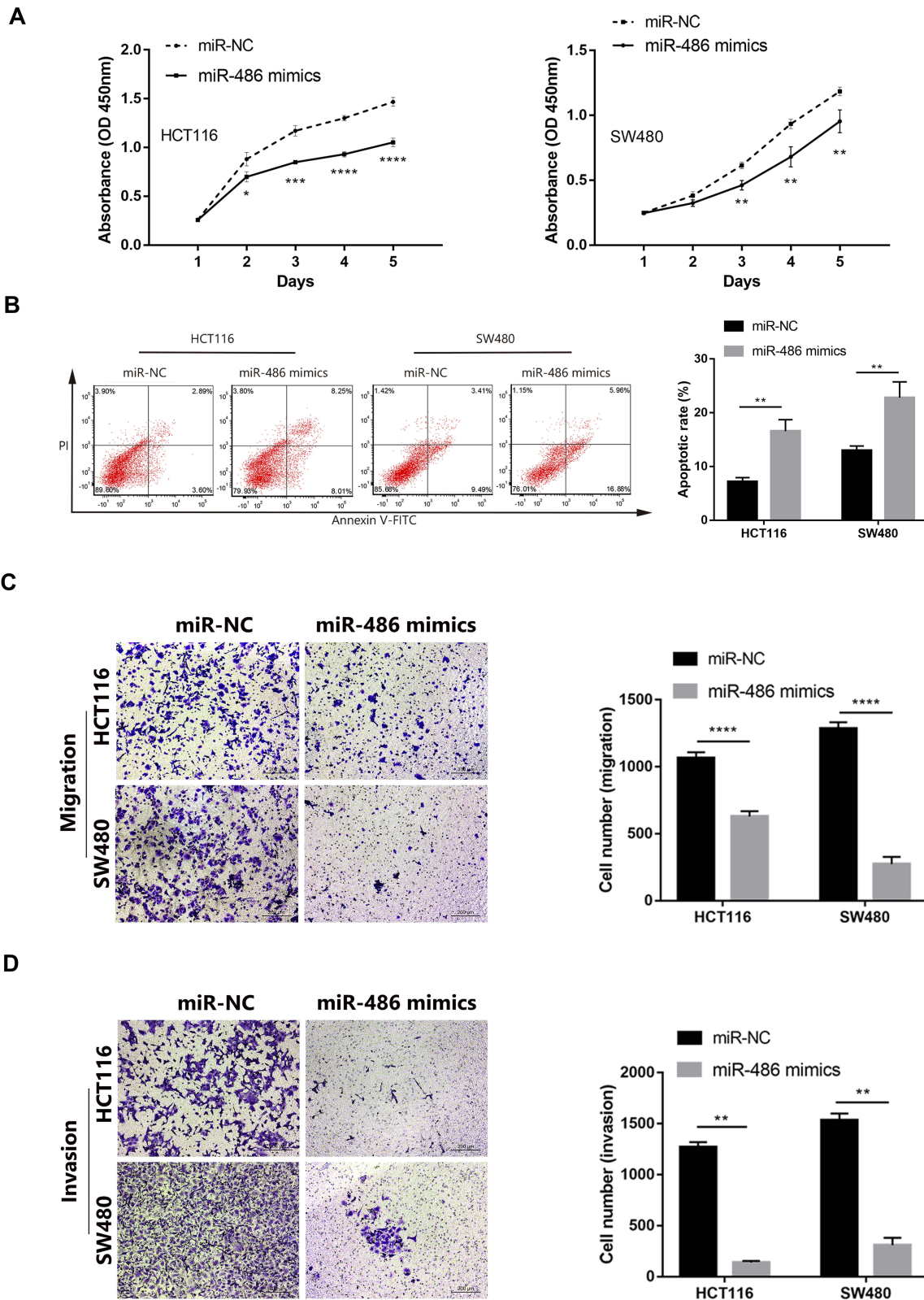
Figure 5 Transfecting miR-486 mimics inhibit the capacity of proliferation, migration, invasion of CRC cells, and promote apoptotic rate in vitro. (**A**) CCK-8 assays showed that the proliferative ability of HCT116 and SW480 cells was significantly inhibited after transfected with miR-486 mimics. (**B**) Flow cytometry suggested HCT116 and SW480 cells showed significantly higher apoptotic rate after transfected with miR-486 mimics. (**C** and **D**) Transwell assays showed that the migration and invasion capacity of HCT116 and SW480 cells were significantly attenuated after transfected with miR-486 mimics. Data are showed as means ± s.d. of at least three independent experiments. *p < 0.05, **p < 0.01 ***p < 0.001, ****p < 0.0001.

432

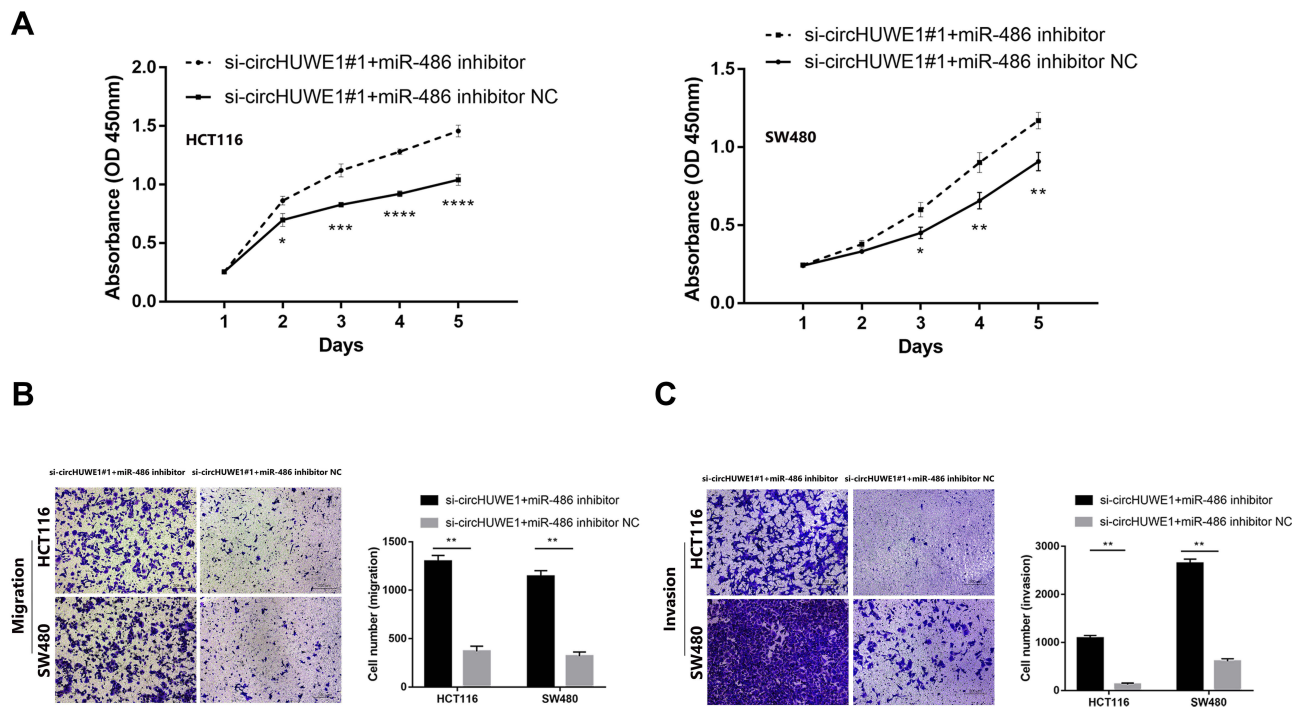OncoTargets and Therapy 2020:13

A

B

C

Figure 6 The tumor-suppressing effect of silencing circHUWE1 could be reversed by miR-486 down-regulation. (**A**) miR-486 inhibitor significantly reversed silencing circHUWE1 mediated supression of proliferation of both HCT116 and SW480 cells. (**B** and **C**) miR-486 inhibitor significantly reversed silencing circHUWE1 mediated supression of migration and invasion of both HCT116 and SW480 cells. *p < 0.05, **p < 0.01, ***p < 0.001, ****p < 0.0001.

by sponging miR-486 and may be a potential therapeutic target for CRC.

Funding

Disclosure

The authors report no conflicts of interest in this work.

References

1. Bray F, Ferlay J, Soerjomataram I, Siegel RL, Torre LA, Jemal A. Global cancer statistics 2018: GLOBOCAN estimates of incidence and mortality worldwide for 36 cancers in 185 countries. *CA Cancer J Clin*. 2018;68(6):394–424. doi:10.3322/caac.21492

2. Li X, Yang L, Chen LL, Biogenesis T. Functions, and challenges of circular RNAs. *Mol Cell*. 2018;71(3):428–442. doi:10.1016/j.molcel.2018.06.034

3. Wilusz JE, Sharp PA. Molecular biology. A circuitous route to non-coding RNA. *Science*. 2013;340(6131):440–441. doi:10.1126/science.1238522

4. Salmena L, Poliseno L, Tay Y, Kats L, Pandolfi PP. A ceRNA hypothesis: the Rosetta stone of a hidden RNA language? *Cell*. 2011;146(3):353–358. doi:10.1016/j.cell.2011.07.014

5. Li Z, Huang C, Bao C, et al. Exon-intron circular RNAs regulate transcription in the nucleus. *Nat Struct Mol Biol*. 2015;22(3):256–264. doi:10.1038/nsmb.2959

6. Ashwal-Fluss R, Meyer M, Pamudurti NR, et al. circRNA biogenesis competes with pre-mRNA splicing. *Mol Cell*. 2014;56(1):55–66. doi:10.1016/j.molcel.2014.08.019

7. Errichelli L, Dini Modigliani S, Laneve P, et al. FUS affects circular RNA expression in murine embryonic stem cell-derived motor neurons. *Nat Commun*. 2017;8:14741. doi:10.1038/ncomms14741

8. Bai Y, Zhang Y, Han B, et al. Circular RNA DLGAP4 ameliorates ischemic stroke outcomes by targeting miR-143 to regulate endothelial-mesenchymal transition associated with blood-brain barrier integrity. *J Neurosci*. 2018;38(1):32–50. doi:10.1523/JNEUROSCI.1348-17.2017

9. Wang K, Long B, Liu F, et al. A circular RNA protects the heart from pathological hypertrophy and heart failure by targeting miR-223. *Eur Heart J*. 2016;37(33):2602–2611. doi:10.1093/eurheartj/ehv713

10. Xu H, Guo S, Li W, Yu P. The circular RNA Cdr1as, via miR-7 and its targets, regulates insulin transcription and secretion in islet cells. *Sci Rep*. 2015;5:12453. doi:10.1038/srep12453

11. Miao R, Wang Y, Wan J, et al. Microarray expression profile of circular RNAs in chronic thromboembolic pulmonary hypertension. *Medicine*. 2017;96(27):e7354. doi:10.1097/MD.0000000000007354

12. Li P, Chen H, Chen S, et al. Circular RNA 0000096 affects cell growth and migration in gastric cancer. *Br J Cancer*. 2017;116(5):626–633. doi:10.1038/bjc.2016.451

13. Han D, Li J, Wang H, et al. Circular RNA circMTO1 acts as the sponge of microRNA-9 to suppress hepatocellular carcinoma progression. *Hepatology*. 2017;66(4):1151–1164. doi:10.1002/hep.29270

14. Luo YH, Zhu XZ, Huang KW, et al. Emerging roles of circular RNA hsa_circ_0000064 in the proliferation and metastasis of lung cancer. *Biomed Pharmacother*. 2017;96:892–898. doi:10.1016/j.biopha.2017.12.015

15. Zheng J, Liu X, Xue Y, et al. TTBK2 circular RNA promotes glioma malignancy by regulating miR-217/HNF1beta/Derlin-1 pathway. *J Hematol Oncol*. 2017;10(1):52. doi:10.1186/s13045-017-0422-2

16. Li XN, Wang ZJ, Ye CX, Zhao BC, Li ZL, Yang Y. RNA sequencing reveals the expression profiles of circRNA and indicates that circDDX17 acts as a tumor suppressor in colorectal cancer. *J Exp Clin Cancer Res*. 2018;37(1):325. doi:10.1186/s13046-018-1006-x

17. Li XN, Wang ZJ, Ye CX, Zhao BC, Huang XX, Yang L. Circular RNA circVAPA is up-regulated and exerts oncogenic properties by sponging miR-101 in colorectal cancer. *Biomed Pharmacother*. 2019;112:108611. doi:10.1016/j.biopha.2019.108611

18. Gong Y, Mao J, Wu D, et al. Circ-ZEB1.33 promotes the proliferation of human HCC by sponging miR-200a-3p and upregulating CDK6. *Cancer Cell Int*. 2018;18:116. doi:10.1186/s12935-018-0602-3

19. Chen S, Li T, Zhao Q, Xiao B, Guo J. Using circular RNA hsa_circ_0000190 as a new biomarker in the diagnosis of gastric cancer. *Clin Chim Acta*. 2017;466:167–171. doi:10.1016/j.cca.2017.01.025

20. Zhao SY, Wang J, Ouyang SB, Huang ZK, Liao L. Salivary circular RNAs Hsa_Circ_0001874 and Hsa_Circ_0001971 as novel biomarkers for the diagnosis of oral squamous cell carcinoma. *Cell Physiol Biochem*. 2018;47(6):2511–2521. doi:10.1159/000491624

21. Zhong Z, Huang M, Lv M, et al. Circular RNA MYLK as a competing endogenous RNA promotes bladder cancer progression through modulating VEGFA/VEGFR2 signaling pathway. *Cancer Lett*. 2017;403:305–317. doi:10.1016/j.canlet.2017.06.027

22. Liu X, Chen X, Zeng K, et al. DNA-methylation-mediated silencing of miR-486-5p promotes colorectal cancer proliferation and migration through activation of PLAGL2/IGF2/beta-catenin signal pathways. *Cell Death Dis*. 2018;9(10):1037. doi:10.1038/s41419-018-1105-9

23. Liu A, Liu L, Lu H. LncRNA XIST facilitates proliferation and epithelial-mesenchymal transition of colorectal cancer cells through targeting miR-486-5p and promoting neuropilin-2. *J Cell Physiol*. 2019;234(8):13747–13761. doi:10.1002/jcp.v234.8

24. Cocquerelle C, Mascrez B, Hetuin D, Bailleul B. Mis-splicing yields circular RNA molecules. *FASEB j*. 1993;7(1):155–160. doi:10.1096/fasebj.7.1.7678559

25. Rybak-Wolf A, Stottmeister C, Glazar P, et al. Circular RNAs in the mammalian brain are highly abundant, conserved, and dynamically expressed. *Mol Cell*. 2015;58(5):870–885. doi:10.1016/j.molcel.2015.03.027

26. Memczak S, Papavasileiou P, Peters O, Rajewsky N, Pfeffer S. Identification and characterization of circular RNAs as a new class of putative biomarkers in human blood. *PLoS One*. 2015;10(10):e0141214. doi:10.1371/journal.pone.0141214

27. Westholm JO, Miura P, Olson S, et al. Genome-wide analysis of drosophila circular RNAs reveals their structural and sequence properties and age-dependent neural accumulation. *Cell Rep*. 2014;9(5):1966–1980. doi:10.1016/j.celrep.2014.10.062

28. Salzman J, Chen RE, Olsen MN, Wang PL, Brown PO. Cell-type specific features of circular RNA expression. *PLoS Genet*. 2013;9(9):e1003777. doi:10.1371/journal.pgen.1003777